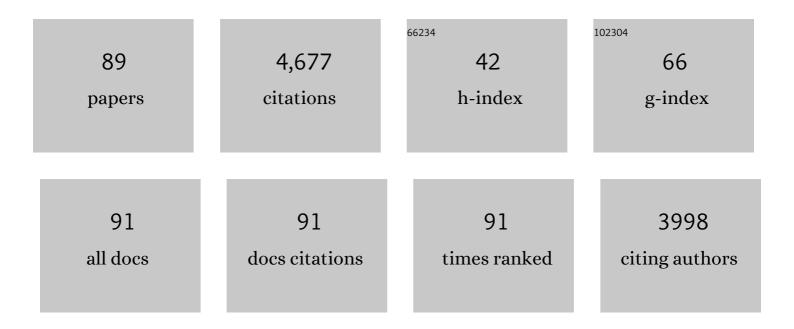
Xiao–Kun Ouyang

List of Publications by Year in descending order

Source: https://exaly.com/author-pdf/6479197/publications.pdf Version: 2024-02-01



#	Article	IF	CITATIONS
1	Fabrication of carboxylated cellulose nanocrystal/sodium alginate hydrogel beads for adsorption of Pb(II) from aqueous solution. International Journal of Biological Macromolecules, 2018, 108, 149-157.	3.6	269
2	Adsorptive removal of cationic methylene blue dye using carboxymethyl cellulose/k-carrageenan/activated montmorillonite composite beads: Isotherm and kinetic studies. International Journal of Biological Macromolecules, 2018, 106, 823-833.	3.6	213
3	Adsorption behavior of carboxylated cellulose nanocrystal—polyethyleneimine composite for removal of Cr(VI) ions. Applied Surface Science, 2017, 408, 77-87.	3.1	194
4	Fabrication of magnetic bentonite/carboxymethyl chitosan/sodium alginate hydrogel beads for Cu (II) adsorption. International Journal of Biological Macromolecules, 2019, 135, 490-500.	3.6	191
5	Fabrication of a Magnetic Cellulose Nanocrystal/Metal–Organic Framework Composite for Removal of Pb(II) from Water. ACS Sustainable Chemistry and Engineering, 2017, 5, 10447-10458.	3.2	154
6	Efficient adsorption of diclofenac sodium from aqueous solutions using magnetic amine-functionalized chitosan. Chemosphere, 2019, 217, 270-278.	4.2	145
7	Fabrication of polyethylenimine-functionalized sodium alginate/cellulose nanocrystal/polyvinyl alcohol core–shell microspheres ((PVA/SA/CNC)@PEI) for diclofenac sodium adsorption. Journal of Colloid and Interface Science, 2019, 554, 48-58.	5.0	128
8	Adsorption of diclofenac sodium on bilayer amino-functionalized cellulose nanocrystals/chitosan composite. Journal of Hazardous Materials, 2019, 369, 483-493.	6.5	119
9	Adsorption of lead ions from aqueous solutions by porous cellulose nanofiber–sodium alginate hydrogel beads. Journal of Molecular Liquids, 2021, 324, 115122.	2.3	118
10	pH-sensitive ZnO/carboxymethyl cellulose/chitosan bio-nanocomposite beads for colon-specific release of 5-fluorouracil. International Journal of Biological Macromolecules, 2019, 128, 468-479.	3.6	117
11	Dual-layered pH-sensitive alginate/chitosan/kappa-carrageenan microbeads for colon-targeted release of 5-fluorouracil. International Journal of Biological Macromolecules, 2019, 132, 487-494.	3.6	104
12	Adsorption of Pb(II) from aqueous solutions using crosslinked carboxylated chitosan/carboxylated nanocellulose hydrogel beads. Journal of Molecular Liquids, 2021, 322, 114523.	2.3	94
13	A novel molecularly imprinted polymer of the specific ionic liquid monomer for selective separation of synephrine from methanol–water media. Food Chemistry, 2013, 141, 3578-3585.	4.2	89
14	Magnetic carboxylated cellulose nanocrystals as adsorbent for the removal of Pb(II) from aqueous solution. International Journal of Biological Macromolecules, 2016, 93, 547-556.	3.6	89
15	Composition and anti-inflammatory effect of polysaccharides from Sargassum horneri in RAW264.7 macrophages. International Journal of Biological Macromolecules, 2016, 88, 403-413.	3.6	87
16	Adsorption of Pb(II) from fish sauce using carboxylated cellulose nanocrystal: Isotherm, kinetics, and thermodynamic studies. International Journal of Biological Macromolecules, 2017, 102, 232-240.	3.6	80
17	Stabilization of zein nanoparticles with k-carrageenan and tween 80 for encapsulation of curcumin. International Journal of Biological Macromolecules, 2020, 146, 549-559.	3.6	80
18	Facile Fabrication of ZIF-8/Calcium Alginate Microparticles for Highly Efficient Adsorption of Pb(II) from Aqueous Solutions. Industrial & Engineering Chemistry Research, 2019, 58, 6394-6401.	1.8	77

Xiao–Kun Ouyang

#	Article	IF	CITATIONS
19	Fabrication of soy protein isolate/cellulose nanocrystal composite nanoparticles for curcumin delivery. International Journal of Biological Macromolecules, 2020, 165, 1468-1474.	3.6	77
20	Development and characterization of soybean protein isolate and fucoidan nanoparticles for curcumin encapsulation. International Journal of Biological Macromolecules, 2021, 169, 194-205.	3.6	77
21	PEI-modified core-shell/bead-like amino silica enhanced poly (vinyl alcohol)/chitosan for diclofenac sodium efficient adsorption. Carbohydrate Polymers, 2020, 229, 115459.	5.1	76
22	Preparation of pH-sensitive Fe3O4@C/carboxymethyl cellulose/chitosan composite beads for diclofenac sodium delivery. International Journal of Biological Macromolecules, 2019, 127, 594-605.	3.6	75
23	Surface-Imprinted Magnetic Carboxylated Cellulose Nanocrystals for the Highly Selective Extraction of Six Fluoroquinolones from Egg Samples. ACS Applied Materials & amp; Interfaces, 2017, 9, 1759-1769.	4.0	73
24	Highly efficient adsorption of Pb(II) from aqueous solution using amino-functionalized SBA-15/calcium alginate microspheres as adsorbent. International Journal of Biological Macromolecules, 2019, 125, 808-819.	3.6	71
25	Fabrication of tetraethylenepentamine functionalized alginate beads for adsorptive removal of Cr (VI) from aqueous solutions. International Journal of Biological Macromolecules, 2019, 125, 1221-1231.	3.6	70
26	Efficient adsorption of Levofloxacin from aqueous solution using calcium alginate/metal organic frameworks composite beads. Journal of Sol-Gel Science and Technology, 2019, 91, 353-363.	1.1	68
27	Fabrication of cross-linked chitosan beads grafted by polyethylenimine for efficient adsorption of diclofenac sodium from water. International Journal of Biological Macromolecules, 2020, 145, 1180-1188.	3.6	68
28	Fabrication of ofloxacin imprinted polymer on the surface of magnetic carboxylated cellulose nanocrystals for highly selective adsorption of fluoroquinolones from water. International Journal of Biological Macromolecules, 2018, 107, 453-462.	3.6	66
29	Polyphenol-based hydrogels: Pyramid evolution from crosslinked structures to biomedical applications and the reverse design. Bioactive Materials, 2022, 17, 49-70.	8.6	64
30	Delivery of curcumin using a zein-xanthan gum nanocomplex: Fabrication, characterization, and in vitro release properties. Colloids and Surfaces B: Biointerfaces, 2021, 204, 111827.	2.5	62
31	Encapsulation of curcumin using fucoidan stabilized zein nanoparticles: Preparation, characterization, and in vitro release performance. Journal of Molecular Liquids, 2021, 329, 115586.	2.3	60
32	Fabrication and characterization of zein-alginate oligosaccharide complex nanoparticles as delivery vehicles of curcumin. Journal of Molecular Liquids, 2021, 342, 116937.	2.3	58
33	Adsorption of Pb(II) from aqueous solution by polyacrylic acid grafted magnetic chitosan nanocomposite. International Journal of Biological Macromolecules, 2020, 154, 1537-1547.	3.6	57
34	Fabrication of novel surface-imprinted magnetic graphene oxide-grafted cellulose nanocrystals for selective extraction and fast adsorption of fluoroquinolones from water. Analytical and Bioanalytical Chemistry, 2017, 409, 6643-6653.	1.9	56
35	Protective effect of polysaccharides from Sargassum horneri against oxidative stress in RAW264.7 cells. International Journal of Biological Macromolecules, 2014, 68, 98-106.	3.6	50
36	Folic Acid and PEI Modified Mesoporous Silica for Targeted Delivery of Curcumin. Pharmaceutics, 2019, 11, 430.	2.0	50

Xiao–Kun Ouyang

#	Article	IF	CITATIONS
37	Chitosan Nanoparticles Attenuate Hydrogen Peroxide-Induced Stress Injury in Mouse Macrophage RAW264.7 Cells. Marine Drugs, 2013, 11, 3582-3600.	2.2	48
38	Facile Preparation of Metal-Organic Framework (MIL-125)/Chitosan Beads for Adsorption of Pb(II) from Aqueous Solutions. Molecules, 2018, 23, 1524.	1.7	47
39	EDTA-functionalized magnetic chitosan oligosaccharide and carboxymethyl cellulose nanocomposite: Synthesis, characterization, and Pb(II) adsorption performance. International Journal of Biological Macromolecules, 2020, 165, 591-600.	3.6	46
40	Preparative separation of four major alkaloids from medicinal plant of Tripterygium Wilfordii Hook F using high-speed counter-current chromatography. Separation and Purification Technology, 2007, 56, 319-324.	3.9	44
41	Shear-Induced Breakup of Cellulose Nanocrystal Aggregates. Langmuir, 2017, 33, 235-242.	1.6	44
42	Efficient adsorption of Pb(II) from aqueous solutions using aminopropyltriethoxysilane-modified magnetic attapulgite@chitosan (APTS-Fe3O4/APT@CS) composite hydrogel beads. International Journal of Biological Macromolecules, 2019, 137, 741-750.	3.6	43
43	Efficient adsorption of Cu(II) from aqueous solutions by acid-resistant and recyclable ethylenediamine tetraacetic acid-grafted polyvinyl alcohol/chitosan beads. Journal of Molecular Liquids, 2020, 316, 113856.	2.3	42
44	Oxidative stress-amplified nanomedicine for intensified ferroptosis-apoptosis combined tumor therapy. Journal of Controlled Release, 2022, 347, 104-114.	4.8	42
45	Enhancing the stability of zein/fucoidan composite nanoparticles with calcium ions for quercetin delivery. International Journal of Biological Macromolecules, 2021, 193, 2070-2078.	3.6	40
46	Fabrication of chitosan-based MCS/ZnO@Alg gel microspheres for efficient adsorption of As(V). International Journal of Biological Macromolecules, 2019, 139, 886-895.	3.6	37
47	Partially Hydrolyzed Bamboo (<i>Phyllostachys heterocycla</i>) As a Porous Bioadsorbent for the Removal of Pb(II) from Aqueous Mixtures. Journal of Agricultural and Food Chemistry, 2014, 62, 6007-6015.	2.4	36
48	Cellulose nanocrystal/calcium alginate-based porous microspheres for rapid hemostasis and wound healing. Carbohydrate Polymers, 2022, 293, 119688.	5.1	36
49	Fabrication of Carboxymethylcellulose/Metal-Organic Framework Beads for Removal of Pb(II) from Aqueous Solution. Materials, 2019, 12, 942.	1.3	33
50	Efficient Adsorption of Pb(II) from Aqueous Solutions by Metal Organic Framework (Zn-BDC) Coated Magnetic Montmorillonite. Polymers, 2018, 10, 1383.	2.0	32
51	Adsorption of Pb(II) from Aqueous Solutions Using Nanocrystalline Cellulose/Sodium Alginate/K-Carrageenan Composite Hydrogel Beads. Journal of Polymers and the Environment, 2022, 30, 1995-2006.	2.4	32
52	High-performance liquid chromatography coupled with electrospray ionization tandem mass spectrometry for the determination of flocoumafen and brodifacoum in whole blood. Journal of Applied Toxicology, 2007, 27, 18-24.	1.4	31
53	Fabrication of Composite Beads Based on Calcium Alginate and Tetraethylenepentamine-Functionalized MIL-101 for Adsorption of Pb(II) from Aqueous Solutions. Polymers, 2018, 10, 750.	2.0	31
54	Viscosity Calculations for Ionic Liquidâ^'Cosolvent Mixtures Based on Eyring's Absolute Rate Theory and Activity Coefficient Models. Journal of Chemical & Engineering Data, 2010, 55, 4878-4884.	1.0	29

#	Article	IF	CITATIONS
55	Fabrication of magnetic carboxyl-functionalized attapulgite/calcium alginate beads for lead ion removal from aqueous solutions. International Journal of Biological Macromolecules, 2018, 120, 789-800.	3.6	29
56	Efficient Delivery of Curcumin by Alginate Oligosaccharide Coated Aminated Mesoporous Silica Nanoparticles and In Vitro Anticancer Activity against Colon Cancer Cells. Pharmaceutics, 2022, 14, 1166.	2.0	29
57	Fabrication of Ion-Crosslinking Aminochitosan Nanoparticles for Encapsulation and Slow Release of Curcumin. Pharmaceutics, 2019, 11, 584.	2.0	28
58	Liquid–liquid extraction of caprolactam from water using room temperature ionic liquids. Separation and Purification Technology, 2013, 104, 263-267.	3.9	24
59	Wetting ofÂsoy protein adhesives modified by urea on wood surfaces. European Journal of Wood and Wood Products, 2012, 70, 11-16.	1.3	23
60	Delivery of curcumin by fucoidan-coated mesoporous silica nanoparticles: Fabrication, characterization, and in vitro release performance. International Journal of Biological Macromolecules, 2022, 211, 368-379.	3.6	23
61	Adsorption of caprolactam from aqueous solution by novel polysulfone microcapsules containing [Bmim][PF6]. Colloids and Surfaces A: Physicochemical and Engineering Aspects, 2014, 441, 72-76.	2.3	21
62	Simultaneous determination of four sesquiterpene alkaloids inTripterygium wilfordii Hook. F. extracts by High-performance liquid chromatography. Phytochemical Analysis, 2007, 18, 320-325.	1.2	18
63	Facile fabrication of core–shell/bead-like ethylenediamine-functionalized Al-pillared montmorillonite/calcium alginate for As(V) ion adsorption. International Journal of Biological Macromolecules, 2019, 131, 971-979.	3.6	18
64	Extraction of Puerarin using Ionic Liquid Based Aqueous Two-Phase Systems. Separation Science and Technology, 2012, 47, 1740-1747.	1.3	17
65	Simultaneous Determination of Triptolide and Tripdiolide in Extract of Tripterygium wilfordii Hook. f. by LC–APCI-MS. Chromatographia, 2007, 65, 373-375.	0.7	16
66	Simultaneous determination of triptolide, tripdiolide and tripterine in human urine by highâ€performance liquid chromatography coupled with ion trap atmosphericâ€pressure chemical ionization mass spectrometry. Biomedical Chromatography, 2009, 23, 289-294.	0.8	16
67	Adsorption of Pb(II) from Aqueous Solution by Mussel Shell-Based Adsorbent: Preparation, Characterization, and Adsorption Performance. Materials, 2021, 14, 741.	1.3	16
68	Synthesis and Characterization of Magnetic Molecularly Imprinted Polymer for the Enrichment of Ofloxacin Enantiomers in Fish Samples. Molecules, 2016, 21, 915.	1.7	15
69	Determination of four pyridine alkaloids from Tripterygium wilfordii Hook. f. in human plasma by high-performance liquid chromatography coupled with mass spectrometry. Journal of Chromatography B: Analytical Technologies in the Biomedical and Life Sciences, 2011, 879, 3516-3522.	1.2	14
70	Bamboo-derived porous bioadsorbents and their adsorption of Cd(ii) from mixed aqueous solutions. RSC Advances, 2014, 4, 28699.	1.7	14
71	Facile fabrication of surface molecularly imprinted magnetic polydopamine for selective adsorption of fluoroquinolone from aqueous solutions. Journal of Molecular Structure, 2021, 1243, 130894.	1.8	14
72	Enzymatic approaches to the preparation of chiral epichlorohydrin. RSC Advances, 2015, 5, 92988-92994.	1.7	12

#	Article	IF	CITATIONS
73	Ion chromatography tandem mass spectrometry for simultaneous confirmation and determination of indandione rodenticides in serum. Biomedical Chromatography, 2009, 23, 1217-1226.	0.8	10
74	Fabrication of porous polyethyleneimine-functionalized chitosan/Span 80 microspheres for adsorption of diclofenac sodium from aqueous solutions. Sustainable Chemistry and Pharmacy, 2021, 21, 100418.	1.6	10
75	Fabrication, characterization, and in vitro evaluation of doxorubicin-coupled chitosan oligosaccharide nanoparticles. Journal of Molecular Structure, 2022, 1268, 133688.	1.8	10
76	Simultaneous Determination of Flumequine and Oxolinic Acid Residues in Aquatic Products Using Pressurized Capillary Electrochromatography. Food Analytical Methods, 2014, 7, 1770-1775.	1.3	9
77	Diethylenetriaminepentaacetic Acid (DPTA)-modified Magnetic Cellulose Nanocrystals can Efficiently Remove Pb(II) from Aqueous Solution. Journal of Polymers and the Environment, 2022, 30, 1344-1354.	2.4	9
78	Development and Validation of a Liquid Chromatography Coupled with Atmospheric-Pressure Chemical Ionization Ion Trap Mass Spectrometric Method for the Simultaneous Determination of Triptolide, Tripdiolide, and Tripterine in Human Serum. Journal of Analytical Toxicology, 2008, 32, 737-743.	1.7	8
79	Validation a solid-phase extraction-HPLC method for determining the migration behaviour of five aromatic amines from packaging bags into seafood simulants. Food Additives and Contaminants - Part A Chemistry, Analysis, Control, Exposure and Risk Assessment, 2014, 31, 1598-1604.	1.1	8
80	Pharmacokinetic study of ofloxacin enantiomers in <i>Pagrosomus major</i> by chiral HPLC. Biomedical Chromatography, 2016, 30, 426-431.	0.8	8
81	Characterization and determination of chlorophacinone in plasma by ion chromatography coupled with ion trap electrospray ionization mass spectrometry. Biomedical Chromatography, 2009, 23, 524-530.	0.8	7
82	Enhancement of epoxide hydrolase production by ⁶⁰ Co gamma and UV irradiation mutagenesis of <i>Aspergillus niger</i> ZJBâ€09103. Biotechnology and Applied Biochemistry, 2017, 64, 392-399.	1.4	7
83	The Simultaneous Production of Two Distinct Types of Cellulose Nanocrystals. Langmuir, 2022, 38, 5996-6003.	1.6	6
84	Rapid Identification and Determination of the Rodenticide Valone in Serum by High-Performance Liquid Chromatography-Tandem Mass Spectrometry. Journal of Analytical Toxicology, 2009, 33, 104-108.	1.7	5
85	Chiral separation and enantioselective degradation of trichlorfon enantiomers in mariculture pond water. Analytical Methods, 2016, 8, 3196-3203.	1.3	5
86	Validation of a Chiral Liquid Chromatographic Method for the Degradation Behavior of Flumequine Enantiomers in Mariculture Pond Water. Chirality, 2016, 28, 649-655.	1.3	3
87	Analysis of flumequine enantiomers in rat plasma by UFLCâ€ESIâ€MS/MS. Chirality, 2016, 28, 737-743.	1.3	2
88	Investigation into the enantiospecific behavior of trichlorfon enantiomers during microorganism degradation. RSC Advances, 2016, 6, 3934-3941.	1.7	1
89	Enantioseparation and enantioselective behavior of trichlorfon enantiomers in sediments. Chirality, 2017, 29, 140-146.	1.3	1